PROCEEDINGS OF SCIENCE

On the resonant and non-resonant effects in the $B \to K^*(\to K\pi)\nu\bar{\nu}$

Diganta Das
Physical Research Laboratory, Navrangpura, Ahmedabad 380 009, India
E-mail: diganta@prl.res.in

We investigate the impacts of resonant and non-resonant backgrounds to $B \to K^*(\to K\pi)\nu\bar{\nu}$ decay. Such effects arise beyond the narrow width approximation of the K^* meson. The non-resonant amplitudes are studied using Heavy-Hadron-Chiral-Perturbation theory in the kinematic region of low hadronic recoil. We find that in the K^* signal window the non-resonant amplitudes induce an uncertainty of about 20% in the branching fraction, and at most few % in the longitudinal polarization fraction F_L. Uncertainties induced by broad scalar resonances K_0^* and κ are at the level of few percents in the branching fraction in the K^* signal window and negligible in longitudinal polarization fraction F_L. Since the effects of background in F_L are small, this observable can be used to test form factors, or alternatively the right-handed currents in the entire q^2-region. We define a new observable, the forward-backward asymmetry $A_{\rm FBL}^K$ that can be used to experimentally constrain the resonant and non-resonant backgrounds.

9th International Workshop on the CKM Unitarity Triangle
28 November - 3 December 2016
Tata Institute for Fundamental Research (TIFR), Mumbai, India

PoS(CKM2016)078

1. Introduction

The $B \to K^*(\to K\pi)\nu\bar{\nu}$ is a rare semi-leptonic decay that is induced by $b \to s\nu\bar{\nu}$ flavor changing neutral current (FCNC) transition which is sensitive to physics beyond the Standard Model (SM). In the past several decades, FCNC transition in $b \to s\ell^+\ell^-$ have been the topic of extensive theoretical and experimental investigations [1, 2]. Unlike $b \to s\ell^+\ell^-$, the $b \to s\nu\bar{\nu}$ is not subject to electromagnetic effects so factorization is exact and the form factors are the only source of hadronic uncertainty in $B \to K^*(\to K\pi)\nu\bar{\nu}$ decay. It is therefore expected to play and important role in searches of new physics in the upcoming B-physics experiments. However, final state neutrinos make it experimentally challenging to measure and the current best upper limit from Belle at 90% confidence level reads [3]

$$\mathscr{B}(B \to K^*\nu\bar{\nu}) < 1.8 \times 10^{-5}, \tag{1.1}$$

which is around the corner of the prediction in the SM. For detailed NP analysis in $b \to s\nu\bar{\nu}$ see Refs. [4, 5, 6, 7, 8]. In this article we study the backgrounds induced by the broad scalar resonances $K_0^*(1430)$ and κ that decay to a $K\pi$ pair and that induced by the non-resonant $B \to K\pi\nu\bar{\nu}$ decay. These effects in $B \to K^*\ell^+\ell^-$ have been studied in [9, 10, 11] and [12, 13] and recently the S-wave fraction in $B \to K^*(\to K\pi)\mu^+\mu^-$ was measured by the LHCb Collaboration [14].

The article is organized as follows. We describe the $b \to s\nu\bar{\nu}$ effective Hamiltonian in Sec. 2. The differential distributions in the presence of resonant and non-resonant modes are worked out in Sec. 3 and we do the numerical analysis in Sec. 4.

2. Effective Hamiltonian

The low energy effective Hamiltonian for $b \to s\nu\bar{\nu}$ transition reads [4, 6]

$$\mathscr{H}_{\rm eff} = -\frac{4G_F}{\sqrt{2}}\lambda_t\frac{\alpha}{8\pi}\Big[(C_L+C_R)(\bar{s}\gamma_\mu b)+(C_R-C_L)(\bar{s}\gamma_\mu\gamma_5 b)\Big]\sum_i \bar{\nu}_i\gamma^\mu(1-\gamma_5)\nu_i + \text{h.c}, \tag{2.1}$$

where α is the electromagnetic coupling constant, $\lambda_t = V_{tb}V_{ts}^*$ and $i = e,\mu,\tau$. In the SM the Wilson coefficient C_L is calculated at the next-to-leading order in perturbative QCD [15, 16] and is given by $C_L = -X(m_t^2/m_W^2)/\sin^2\theta_W$ where the loop function is $X(m_t^2/m_W^2) = 1.469 \pm 0.017$ [17]. The right handed coupling C_R is zero in the SM but arise in the extensions of SM.

3. The resonant and non-resonant contributions to $B \to K^*(\to K\pi)\nu\bar{\nu}$

In our notation, the four-momentum of B, K^*, K, π are p_B, k, p_K and p_π, respectively, and the four-momentum of neutrino and the anti-neutrino are p_ν and $p_{\bar{\nu}}$. The angle between the kaon and the opposite direction of B in the $K\pi$ rest frame is defined as θ_K. We work in the transversity basis where the three transversity amplitudes in the narrow width approximation (NWA) of the K^* are denoted by $H_{\perp,\parallel,0}$. The detailed expressions of $H_{\perp,\parallel,0}$ in terms of the $B \to K^*$ form factors $V(q^2), A_{0,1,2}(q^2)$, where $q = p_\nu + p_{\bar{\nu}}$, are given in Ref. [18]. For our numerical analysis we use the form factors given in Ref. [19] that were obtained from the combined fit to the results calculated in the light-cone sum rules (LCSR) [19] and in the Lattice QCD [20].

In this work, we go beyond the NWA of the K^* by parameterizing its propagator by Breit-Wigner type ansatz and re-writing the transversity amplitudes as $\widetilde{H}_{0,\parallel,\perp}(q^2,p^2)$, where $p = p_K + p_\pi$. As we go beyond the NWA we include the contributions of broad intermediate scalars $K_0^*(1430)$ and κ that decay to $K\pi$ pair and the contributions four body non-resonant $B \to K\pi\nu\bar{\nu}$ mode. For simplicity we will denote both $K_0^*(1430)$ and κ as K_0^*.

The $B \to K\pi$ form factors are known from calculations in Heavy-Hadron-Chiral-Perturbation-Theory (HHχPT) [21] expected to be valid in the region where $p_B.p_{K,\pi}/m_B \lesssim 1$GeV which is satisfied in the high-q^2 region. We take the $B \to K_0^*$ form factors from QCD-sum-rules calculations [22] which is valid in the low-q^2 region. To this end in Sec. 4 we perform our analysis in two q^2 regions, "low-q^2" corresponds to [0-14]GeV^2 and "high-q^2" corresponds to [14-19]GeV^2.

Adding the amplitudes of three contributions we get the three-fold differential distribution as

$$\frac{d^3\Gamma}{dq^2 dp^2 d\cos\theta_K} = \frac{3N(q^2)|\vec{q'}||\vec{p'}_K|}{3\times 8(2\pi)^5 m_B^2\sqrt{p^2}}\Big[|e^{-i\delta}\widetilde{H}_\perp + H_\perp^{\rm nr}|^2 + |e^{-i\delta}\widetilde{H_\parallel} + H_\parallel^{\rm nr}|^2 + |e^{-i\delta}\widetilde{H_0} + H_0^{\rm nr} + e^{-i\delta}\widetilde{H_0}'|^2\Big]. \tag{3.1}$$

In the numerator of the above equation, the factor of three correspond to summation of three flavors of the final state neutrinos. Here $H^{\rm nr}_{0,\parallel,\perp}(q^2,p^2)$ are the transversity amplitudes of the non-resonant mode while $\widetilde{H}'_0(q^2,p^2)$ denote the transversity amplitudes of the $B \to K_0^*(\to K\pi)\nu\bar{\nu}$ for finite width of the K_0^* [18]. The expressions of $|\vec{q'}|, |\vec{p'}_K|$ are defined in [18]. Here we have introduced a relative strong phase δ between the resonant and the non-resonant modes. We define the longitudinal polarization fraction F_L and its q^2-averaged version $\langle F_L\rangle$ as

$$F_L = \frac{d\Gamma_L/dq^2}{d\Gamma/dq^2}, \quad \langle F_L\rangle = \frac{\int_{q^2_{\rm min}}^{q^2_{\rm max}} d\Gamma_L/dq^2}{\int_{q^2_{\rm min}}^{q^2_{\rm max}} d\Gamma/dq^2}. \tag{3.2}$$

In addition, we define the forward-backward asymmetry $A^K_{\rm FB}$, or alternatively, $A^K_{\rm FB\,L}$ as

$$A^K_{\rm FB\,(L)} \equiv \frac{\int_0^1 d\cos\theta_K \frac{d^2\Gamma}{dq^2 d\cos\theta_K} - \int_{-1}^0 d\cos\theta_K \frac{d^2\Gamma}{dq^2 d\cos\theta_K}}{\Gamma_{(L)}}, \tag{3.3}$$

where Γ_L is the longitudinal decay rate defined in [18]. These observables are studied in the next section

4. Numerical Analysis

We perform our analysis in two different regions of p^2, P-cut within $[(m_{K^*}-0.1\,\text{GeV})^2, (m_{K^*}+0.1\,\text{GeV})^2]$ and S+P-cut within $[(m_K+m_\pi)^2, 1.44\,\text{GeV}^2]$. For a fixed p^2, the q^2 end point is a function of p^2, that is $q^2_{\rm max} = (m_B - \sqrt{p^2})^2$. We begin with by calculating the branching ratio and the F_L in the NWA of the K^* in the absence of any backgrounds. Integrating in the full q^2 region [0-19]GeV^2 we find

$$\mathscr{B}(B \to K^*\bar{\nu}\nu) = (9.49 \pm 1.01)\times 10^{-6}, \qquad \langle F_L\rangle = 0.49 \pm 0.04, \tag{4.1}$$

which are consistent with [5, 8, 17]. For the pure $B \to K^*(\to K\pi)\nu\bar{\nu}$ at finite width, the differential branching ratio and the F_L are shown in Fig. 1. The bands correspond to the uncertainties coming from the $B \to K^*$ from factors and input parameters. In the first two rows of Tab. 1 we show the values of q^2 integrated branching ratio in the NWA and for finite width of the K^* with P- and S+P-cuts. The q^2 integrated values of F_L do not differ between P- and S+P-cut for finite width of the K^* and in NWA. Our predictions read $F_L = 0.54 \pm 0.04$ for low-q^2 and $F_L = 0.34 \pm 0.02$ for high-q^2 where errors correspond to the uncertainties in $B \to K^*$ and parametric inputs.

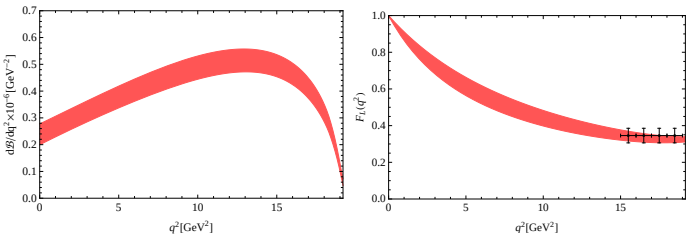

Figure 1: Shown are the differential branching fraction (on the left) and longitudinal polarization fraction F_L (on the right) for pure $B \to K^*(\to K\pi)\nu\bar{\nu}$ as a function of q^2 for p^2 in the P-cut. The error bands correspond to the uncertainties due to the $B \to K^*$ form factors and parametric inputs. The data points in black correspond to form factor calculations in lattice QCD [20, 23].

The effects of the intermediate scalar states are shown in Fig. 2 as the ratio of pure $B \to K^*(\to K\pi)\nu\bar{\nu}$ branching ratio and branching ratio that additionally includes $B \to K_0^*(\to K\pi)\nu\bar{\nu}$ for P- and S+P-cuts. The scalar backgrounds induced uncertainties are at most few percents in P-cut and at most $\sim 10\%$ in the S+P-cut. We find that such effects are negligible in the longitudinal polarization fraction. Note that we refrain from studying the impacts of the scalar resonances at high-q^2 as it would require extrapolation of the scalar form factor into the highly off-shell region for the scalar resonances. In the third row of Tab. 1 we show the low-q^2 integrated branching ratio involving both K^* and K_0^*. The ranges shown correspond to the minimal and maximal values obtained by varying the scalar form factor and input parameters related to the scalar amplitude only. The forward-backward asymmetry $A^K_{\mathrm{FB(L)}}$ which is shown in Fig. 2 is induced by the interference of the K^* with intermediate scalars can be used to test the model of the scalar contribution.

In Fig. 3 we show the ratio of branching ratio and F_L involving the vector meson K^* and the non-resonant mode, normalized by the pure K^* mode as a function of the relative strong phase δ in the high-q^2 region. Both the numerator and the denominator of the ratios are separately integrated over high-q^2 and in P- and S+P-cuts. As can be seen from the figures the strong phase induces an uncertainty up to 20% in the branching ratio for P-cut and about 2.5% in longitudinal polarization fraction. In the last row of Tab. 1 we show the high-q^2 integrated branching ratio involving the K^* and the non-resonant mode. The first errors correspond to the uncertainties coming from the $B \to K^*$ from factors and and the last errors correspond mostly to the unknown strong phase. Our prediction for longitudinal polarization is $\langle F_L \rangle (B \to (K^* + \mathrm{nonres})(\to K\pi)\nu\bar{\nu})|_{\mathrm{P-,S+P-cut}} = 0.34 \pm 0.02 \pm 0.01$, where the first error correspond to the uncertainties coming from the $B \to K^*$ form factors while the second errors correspond to the uncertainties coming from the $B \to K\pi$ from factors and the relative strong phase. Also shown in Fig. 3 is the forward-backward asymmetry $A^K_{\mathrm{FB\ L}}$ which can be used to constrain the strong phase [18].

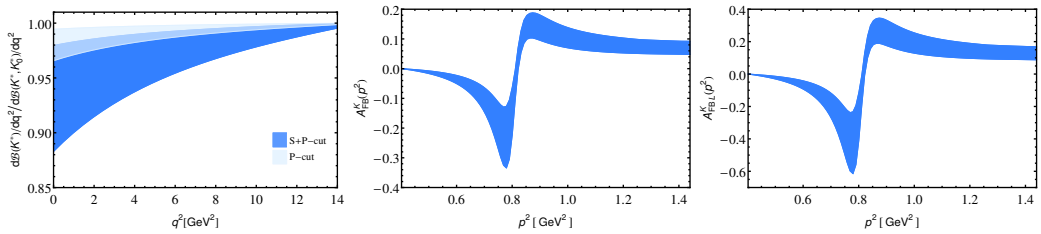

Figure 2: Left: The ratio of differential branching ratios involving only the K^* meson and the differential branching ratio that additionally involves intermediate scalar resonances. Middle (Right): The forward-backward asymmetry $A^K_{\rm FB}(p^2)$ ($A^K_{\rm FB\,L}(p^2)$) as a function of p^2 in the low-q^2 region. The corresponding decay rate(see Eq. 3.3) have been obtained by integrating in the low-q^2 region and p^2 in the S+P-cut.

	$q^2 \in [0-14]\,\text{GeV}^2$	$q^2 \in [14-19]\,\text{GeV}^2$
$\mathscr{B}(B \to K^*\nu\bar{\nu})\vert_{\rm NWA}$	6.96 ± 0.76	2.50 ± 0.22
$\mathscr{B}(B \to K^*(\to K\pi)\nu\bar{\nu})\vert_{\rm P-cut}$	6.01 ± 0.65	2.09 ± 0.22
$\mathscr{B}(B \to K^*(\to K\pi)\nu\bar{\nu})\vert_{\rm P+S-cut}$	6.80 ± 0.73	2.29 ± 0.23
$\mathscr{B}(B \to (\kappa, K_0^*)(\to K\pi)\nu\bar{\nu})\big\vert_{\rm P-cut}$	$[0.01 \ldots 0.07]$	–
$\mathscr{B}(B \to (\kappa, K_0^*)(\to K\pi)\nu\bar{\nu})\big\vert_{\rm S+P-cut}$	$[0.04 \ldots 0.30]$	–
$\mathscr{B}(B \to (K^* + \text{nonres})(\to K\pi)\nu\bar{\nu})\vert_{\rm P-cut}$	–	$2.09 \pm 0.22^{+0.56}_{-0.29}$
$\mathscr{B}(B \to (K^* + \text{nonres})(\to K\pi)\nu\bar{\nu})\vert_{\rm S+P-cut}$	–	$2.29 \pm 0.23^{+0.77}_{-0.27}$

Table 1: The SM branching fractions (in units of 10^{-6}) in low- and high-q^2 and for different cuts in p^2. See texts for details.

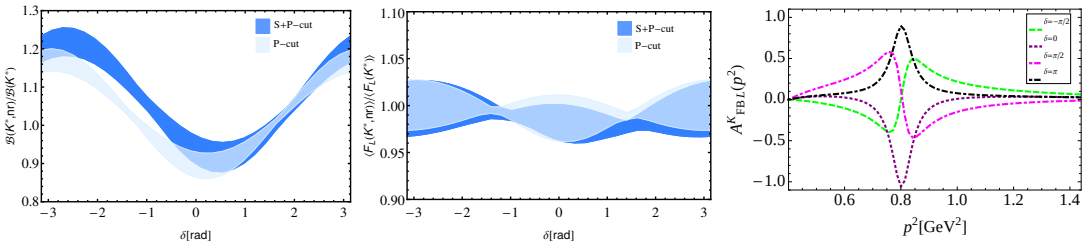

Figure 3: Left(Middle) :The ratio between the branching ratio ($\langle F_L \rangle$) involving intermediate vector meson K^* and non-resonant mode and the branching ratio ($\langle F_L \rangle$) involving the intermediate vector meson K^* only as a function of the relative strong phase δ for p^2 in the P- and S+P-cut. The bands correspond to the uncertainties coming from the non-resonant form factors only. Right: The forward-backward asymmetry $A_{\rm FBL}(p^2)$ for different values of the relative strong phase.

5. Conclusions

We have investigated the $B \to K^*(\to K\pi)\nu\bar{\nu}$ decay and its uncertainties induced by the broad intermediate scalar resonances $K_0^*(1430)$, κ that decay to $K\pi$ final states, and that induced by the non-resonant four body decay $B \to K\pi\nu\bar{\nu}$. These effects are important beyond the NWA of the vector meson K^*. The current availability of the $B \to (K_0^*, \kappa)$ and $B \to K\pi$ form factors restrict us to study the effects separately in the low- and high-q^2 regions. At low-q^2, the contributions of the scalar resonances on branching ratio are at most of the order 1% in the P-cut and $\lesssim 4\%$ in the

S+P-cut. However, the impacts of scalar resonances on the longitudinal polarization fraction F_L is negligible. On the other hand, at high-q^2 the non-resonant contributions to the uncertainty in branching ratio is of $\mathcal{O}(0.1)$ and few % in F_L. These uncertainties can be reduced with a better knowledge of form factors and line shapes. Additionally, the forward-backward asymmetry $A^K_{\text{FB L}}$ can be used to experimentally constrain hadronic backgrounds irrespective of the short distance model.

6. Acknowledgements

My warm thanks go to the organizers of CKM2016. I also thank Gudrun Hiller and Ivan Nišandžić for collaboration on the project [18].

References

[1] T. Blake, T. Gershon and G. Hiller, Ann. Rev. Nucl. Part. Sci. **65** (2015) 113

[2] T. Blake, G. Lanfranchi and D. M. Straub, arXiv:1606.00916 [hep-ph].

[3] P. Goldenzweig, talk for the Belle collaboration at CKM 2016, Mumbai, India, Nov 28- Dec 2, 2016.

[4] P. Colangelo, F. De Fazio, P. Santorelli and E. Scrimieri, Phys. Lett. B **395** (1997) 339

[5] G. Buchalla, G. Hiller and G. Isidori, Phys. Rev. D **63**, 014015 (2000)

[6] W. Altmannshofer, A. J. Buras, D. M. Straub and M. Wick, JHEP **0904** (2009) 022

[7] M. Bartsch, M. Beylich, G. Buchalla and D.-N. Gao, JHEP **0911** (2009) 011

[8] A. J. Buras, J. Girrbach-Noe, C. Niehoff and D. M. Straub, JHEP **1502** (2015) 184

[9] D. Becirevic and A. Tayduganov, Nucl. Phys. B **868** (2013) 368 [arXiv:1207.4004 [hep-ph]].

[10] J. Matias, Phys. Rev. D **86** (2012) 094024 [arXiv:1209.1525 [hep-ph]].

[11] T. Blake, U. Egede and A. Shires, JHEP **1303** (2013) 027 [arXiv:1210.5279 [hep-ph]].

[12] D. Das, G. Hiller, M. Jung and A. Shires, JHEP **1409**, 109 (2014)

[13] D. Das, G. Hiller and M. Jung, arXiv:1506.06699 [hep-ph].

[14] R. Aaij *et al.* [LHCb Collaboration], JHEP **1611**, 047 (2016) [arXiv:1606.04731 [hep-ex]].

[15] G. Buchalla and A. J. Buras, Nucl. Phys. B **548** (1999) 309

[16] M. Misiak and J. Urban, Phys. Lett. B **451** (1999) 161

[17] J. Girrbach-Noe, arXiv:1410.3367 [hep-ph].

[18] D. Das, G. Hiller and I. Nisandzic, arXiv:1702.07599 [hep-ph], to appear in Phys. Rev. D.

[19] A. Bharucha, D. M. Straub and R. Zwicky, JHEP **1608**, 098 (2016)

[20] R. R. Horgan, Z. Liu, S. Meinel and M. Wingate, PoS LATTICE **2014**, 372 (2015)

[21] C. L. Y. Lee, M. Lu and M. B. Wise, Phys. Rev. D **46** (1992) 5040.

[22] T. M. Aliev, K. Azizi and M. Savci, Phys. Rev. D **76**, 074017 (2007)

[23] R. R. Horgan, Z. Liu, S. Meinel and M. Wingate, Phys. Rev. D **89** (2014) no.9, 094501